# Discrete Multi-tone Format for Repeater-Less Direct-Modulation Direct-Detection over 150 km

Zhixin Liu, *Member, IEEE*, Brian Kelly, John O'Carroll, Richard Phelan, David J. Richardson, *Fellow, IEEE*, and Radan Slavík, Senior *Member, IEEE*

***Abstract* — High-capacity and low-cost repeater-less transmission beyond 50 km is of interest for the next-generation inter-data center communications. Transmission over such relatively long distance generally requires transmission in the 1550-nm low-loss telecom band that is, however, impaired by chromatic dispersion. Here, we study the performance of the direct modulation direct detection (DM-DD) system using the discrete multi-tone (DMT) format for repeater-less transmission through up to 150 km of a standard single mode fiber (SMF-28) using the 1550-nm band. The achievable capacity for two different types of directly modulated lasers is studied experimentally and compared with that achievable using chirp-free modulation using a push-pull $LiNbO_3$ Mach-Zehnder external modulator (MZM). The benefit of using a larger bandwidth signal is found to diminish as the transmission distance increases. 28 and 25 Gbit/s signal transmission (Bit Error Ratio, BER < $3.8\times10^{-3}$) over 50 km and 75 km are achieved using just 8-GHz modulation-bandwidth.**

***Index Terms*— Directly modulated laser, Direct detection, Discrete multi-tone, Digital to analog convertor.**

## I. Introduction

TODAY'S Internet has to deal with ever increasing data traffic, which is generated by activities such as ubiquitous multimedia content delivery and online gaming. The key infrastructure that supports these services consists of data centers and Content Delivery Networks (CDNs, i.e., large distributed systems of servers deployed in multiple data centers across the Internet) [1]. These data centers and CDNs require an ever increasing number of short-to-medium reach fiber optic links, continuously pushing optical transceiver technology towards lower power consumption, smaller form factor, and ultimately lower cost-per-bit [2].

Direct-modulation direct-detection (DM-DD) systems using high-order modulation formats are becoming increasingly attractive to address the above-mentioned issue [3-8]. They offer large capacities (e.g., 117 Gbit/s [4]) with minimum optical hardware (e.g., directly modulated laser at the transmitter side and a single photodiode at the receiver side), promising both a low-cost and compact solution. Although direct laser modulation inevitably introduces frequency chirp, novel laser technologies and powerful digital signal processing (DSP) can cope with this to a certain degree. For example, 40 km transmission with >25 Gbit/s data capacities reported recently [9,10] are well suited for inter data center interconnection.

To achieve high-capacity DM-DD transmission, various modulation formats have been proposed, including multi-level Pulse Amplitude Modulation (PAM) [8,11], half-cycle Quadrature Amplitude Modulation (QAM) [12], and Discrete Multi-Tone (DMT) [3-7]. In particular, the DMT modulation format is considered a promising technique because it offers high spectral efficiency and the capability to adapt to component imperfections (e.g., high-frequency modulation roll-off) and transmission impairments. This is particularly relevant in data center applications or standard fiber (SMF-28) based transmission systems impacted by chromatic dispersion-induced frequency fading [3, 13].

However, there are also challenges when implementing DMT, especially in respect to simpler modulation formats like OOK and PAM [8,11,14]. Firstly the cost and power consumption of the DSP is higher for DMT compared to PAM. Another important challenge is the fact that DMT requires a digital-to-analogue convertor (DAC) on the transmitter side and an analogue-to-digital convertor (ADC) on the receiver side, adding cost and power consumption that both scale up with the required bandwidth and effective number of bits (ENOB) [15]. For example, the 100 Gbit/s DM-DD transmission experiment described in ref. [4] required a DAC of the state-of-the-art 20 GHz bandwidth and an ENOB of ~6.5.

Currently, inter data center connections typically range from 10 to 40 km [9,10]. When considering DM-DD for this length range, transmission within the 1310-nm spectral band is the natural choice, as there is close-to-zero dispersion and acceptable (~0.4 dB/km) transmission loss. As a result, most of the work today has concentrated on this telecom band [3,4]. However, as we discussed earlier, longer-distances (e.g. from 50 km to 150 km) are expected to be needed in the future, as newly-planned cloud data centers and CDNs [16] are bigger than those in operation now. For these transmission distances, we expect the transmission loss at 1310 nm to cause more penalty than the chromatic dispersion present in the low-loss 1550-nm window.

In this paper, we study the DMT-based DM-DD system

Manuscript submitted on Oct 27, 2015.

The authors are with the Optoelectronics Research Centre, University of Southampton, Southampton, United Kingdom, SO17 1BJ (e-mail: z.liu@soton.ac.uk).

B. Kelly, R. Phelan, and J. O'Carroll are with Eblana Photonics, Dublin, Ireland.

This research has been supported by EPSRC Fellowship grant agreement no. EP/K003038/1 and EPSRC grant Photonics Hyperhighway, no. EP/I061196X. The data are available through the University of Southampton research depository (DOI: …..)

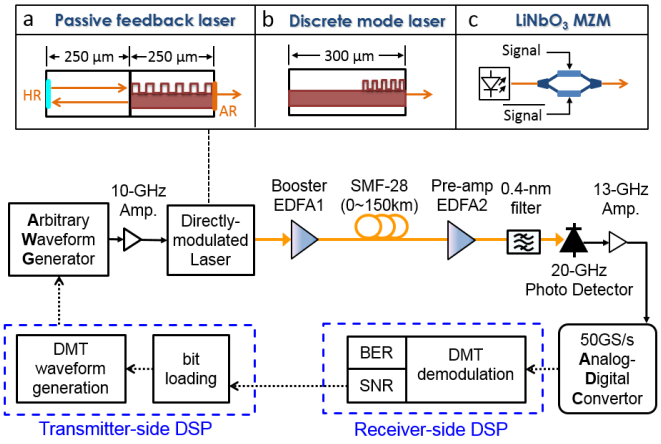


Fig. 1. Experimental setup.

considering transmission beyond 40 km in the low-loss 1550-nm band. First, we study the limitations in the achievable capacity due to the dispersive propagation and the modulation chirp. Further, we pay attention to the achievable capacity as a function of the bandwidth of the electronics used, which influences the system power consumption and cost.

The paper is organized as follows. In Section II we discuss our experimental setup. To evaluate limitations due to the modulation chirp and optical noise, we compare the results obtained with a $LiNbO_3$ Mach-Zehnder modulator (MZM) with two monolithic (and thus potentially low-cost) directly-modulated lasers: a passive feedback laser (PFL) [17] (modulation bandwidth of 34 GHz), and a discrete mode laser (DML) [18,19] (modulation bandwidth of 8.6 GHz). We test them in repeater-less transmission experiments through up to 150 km of SMF-28. In Section III we optimize the back-to-back performance, studying the influence of the DAC resolution, digital pre-emphasis level in the DAC used to compensate for the high-frequency roll-off due to the limited bandwidth of the devices tested, and the number of sub-carriers in the DMT which influences the DSP complexity. In Section IV we show the transmission results.

## II. Experimental Setup

Our experimental setup is shown in Fig.1. The two EDFAs used (one at the transmitter and one at the receiver side) could be eliminated in a field implementation, as we discuss later. The optical power sent to the transmission fiber was 13 dBm. The optical power at the receiver photodiode was kept at 2 dBm. The receiver consisted of a 0.4-nm bandpass filter, 20-GHz photodiode, and a 23-dB gain 13-GHz-bandwidth RF amplifier. The signal was sampled by an 8-bits (nominal) ADC at 50 GSa/s (Tektronix DSA72004) and demodulated using offline DSP.

The DMT waveform samples were generated offline based on a PRBS of $2^{18}$-1 length. To find the optimum number of subcarriers, different inverse discrete Fourier transform (IDFT) sizes (64, 128, …4096) were used for generating the baseband Orthogonal Frequency Division Multiplexing (OFDM) signals. The modulation format for each sub-carrier was assigned by the bit loading algorithm [20,21]. A 1.6% cyclic prefix was placed both before and after each symbol. A clipping ratio of 3.2 (the ratio of the clipping level to the root mean square value) was used.

DMT signals of different bandwidth (2.5, 5 and 8 GHz) were generated by digitally up converting the baseband OFDM signals to 1.25, 2.5 and 4 GHz RF carrier frequencies, respectively, creating real-valued DMT samples. A 10-bit (nominal) arbitrary waveform generator (AWG) operating at 12 GSa/s (not-interleaved) or 24 GSa/s (interleaved) (Tektronix AWG7122C (9.6 GHz bandwidth)) was used to generate the electrical DMT signals. The impact of the DAC resolution was studied by quantizing the DMT samples to a limited number of levels in the transmitter-side DSP software.

The bit loading [21] was calculated using a QPSK-DMT probe with identical power on all sub-carriers. The bit loading for each subcarrier was coarsely determined by measuring the probe signal-to-noise ratio and fine adjustment was made using dynamic bit adaptation. Our modified bit-loading algorithm based on ref. [20] maximized the total capacity at a BER target of $3.8\times10^{-3}$. The BER was calculated using error counting of the demodulated signal.

The structures of the used lasers and the setup with the external MZM are shown as insets a, b, and c in Fig.1. The first laser tested was a 1549-nm pigtailed PFL which consisted of an active distributed feedback (DFB) section and a passive feedback section [17]. Exploiting the self-injection photon-photon resonance, a 3-dB modulation bandwidth of up to 34 GHz was reported for this laser. The laser gain section was biased at 60 mA and the feedback section current was 1.8 mA, simultaneously providing both a small chirp and a flat modulation response [17]. The RF drive signal was amplified to a peak-to-peak voltage of 2.5 V using a 10-GHz bandwidth RF amplifier. The output power of the PFL was 3 dBm. The other laser was a 1548-nm DML [18,19]. The key advantage of this laser is its low fabrication cost (the fabrication process is simpler than for the widely used DFB lasers). Another advantage as compared to a DFB laser is its smaller modulation chirp [22]. The DML was biased at 43 mA and the RF drive signal was 2.2 V (peak-to-peak) and had a package-limited 3-dB bandwidth of 8.6 GHz. The output power of the DML was 4.5 dBm.

## III. Back-to-Back Performance

### A. *Impact of DAC resolution*

We firstly optimized the DMT performance for back-to-back conditions. As the back-to-back performance using either of the two lasers under test was almost identical, we show here only the results obtained with the PFL. Fig. 2a shows the impact of DAC resolution (NOB, number of bits) and sampling rate using the bandwidths of 2.5, 5, and 8 GHz, respectively, using a fixed IDFT size of 1024. Here we see that capacity increases with the DAC resolution (NOB), however, above 6 bits, the capacity increases by only 5-10% when a DAC with 10 bits is used. This suggests that impairments like modulation non-linearity, electronic noise, and receiver-side ADC quantization noise

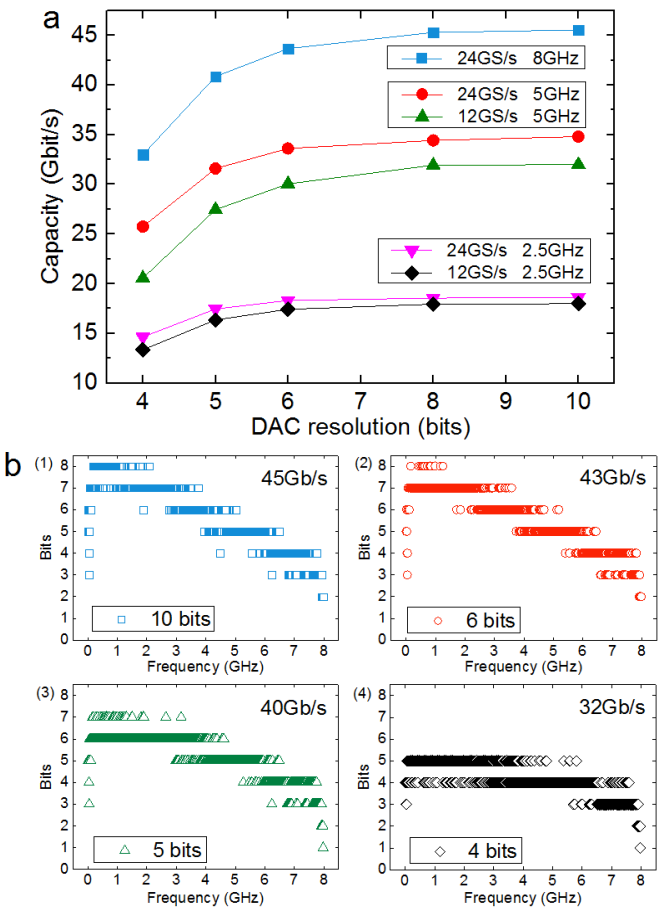


Fig. 2. (a) Back-to-back capacity obtained with different DAC resolutions and sampling rates. (b) Bit allocation map for 8-GHz DMT signal with different DAC resolutions. b(1): 10 bits; b(2): 6 bits; b(3) 5 bits; b(4) 4 bits.

become dominant over the DAC quantization noise when the DAC has more than 6 bits of resolution. Therefore, a 6-bit DAC should be sufficient for cost-sensitive DMT applications. The bit allocation map for 8-GHz bandwidth signal and various levels of DAC resolution is shown in Fig. 2b. When using DAC resolution of 6 bits and more, we achieved modulation format up to 256 QAM in the low frequency region (0-2GHz), where the DAC performance ( high effective number of bits (ENOB)) is the best. Due to the frequency roll-off of all the electronics components involved (DAC, RF amplifiers, photodetector, and DAC) the spectrum efficiency of each subcarrier decreases as frequency increases.

Our results also show that a higher DAC sampling rate (24 GSa/s vs. 12 GSa/s) has negligible impact on a 2.5 GHz system and led to about 10% capacity improvement for a 5 GHz bandwidth system. 12 GSa/s was insufficient (below the Nyquist rate) for 8 GHz and thus was not used.

### *B. Impact of digital pre-emphasis*

The sample-and-hold RF circuit in a DAC introduces significant frequency roll-off in the generated signal (significantly steeper than that due to the limited AWG analog bandwidth), thereby resulting in a decrease of signal-to-noise ratio (SNR) and thus also ENOB in the high frequency region. Previously, we have shown that compensation of the frequency

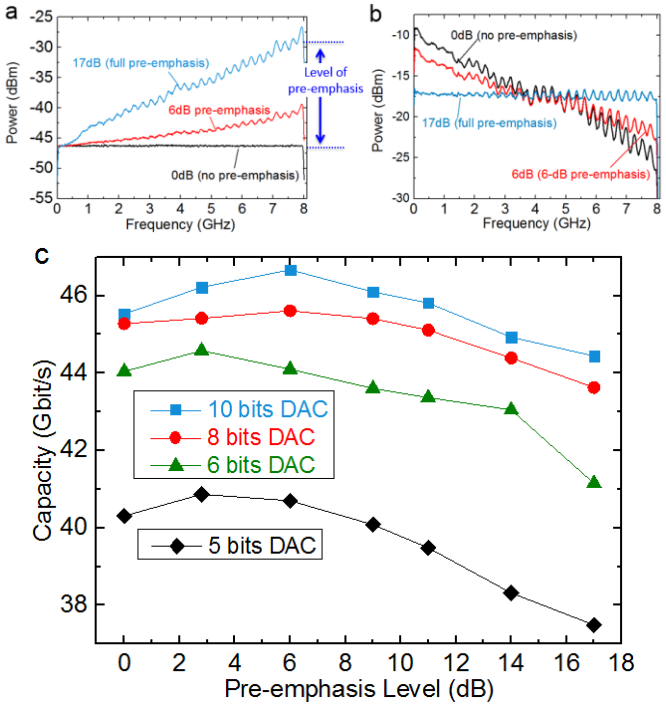


Fig. 3. (a) RF spectrum of the input DMT signal with different pre-emphasis levels. (b) Measured RF spectra of received signals. (c) Back-to-back capacity at different pre-emphasis levels for different DAC resolutions.

roll-off using digital pre-emphasis is of limited value for a 6-bit DAC [13]. Here, we extend this study to include also the impact of the DAC resolution that limits the SNR of the subcarriers. The pre-emphasis level is defined as the power gain applied to the highest frequency signal component with respect to the low frequency components. Fig. 3a shows the spectra of the generated DMT signals generated in the digital domain after applying pre-emphasis levels of 0, 6, and 17 dB, respectively. The corresponding RF spectra obtained after reception are shown in Fig. 3b. The 17 dB frequency roll-off from DC to 8 GHz and the ripples are mainly due to the limited bandwidth and DAC interleaving, respectively.

Fig. 3c shows the maximum achievable capacity as a function of the pre-emphasis level using different DAC resolutions. The highest capacity is achieved with a modest level of pre-emphasis (4-6 dB), giving only slightly better performance (<3 % in capacity) than that obtained with no pre-emphasis. This negligible benefit together with the fact that the pre-emphasis requires power and resources-consuming DSP suggests to not use pre-emphasis.

### *C. Impact of the number of subcarriers*

Fig. 4 shows the capacity obtained as a function of subcarrier numbers for DMT signals of 5, and 8 GHz bandwidth. We see that the achieved capacities increase with the number of subcarriers because it allows a finer granular adaptation to channel conditions. However, a larger number of subcarriers also requires larger computational power. In what follows, we use 1024 sub-carriers that results in capacity penalty of ~2%, but requires less computational power than using 4096 subcarriers. Compared to the results in [23], which showed 12-

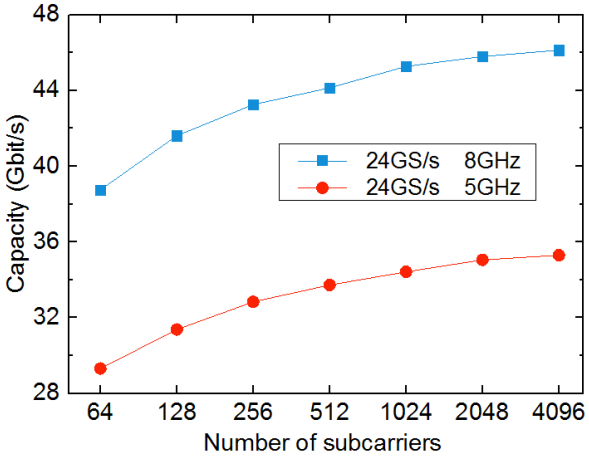


Fig. 4. Capacity obtained for DMT signal with different number of subcarriers. Signals were generated using 8-bits 24-GSa/s DAC without pre-emphasis.

GHz bandwidth DMT signal with a 24 GS/s DAC, our results show a slower decrease of capacity when decreasing the number of subcarriers. We believe this is due to the smaller signal bandwidth used in our experiment.

## IV. Transmission Results

Based on the back-to-back analysis shown in the previous section, we use 8-bits DAC resolution, 24 GSa/s sampling rate, 1024 subcarriers, and no pre-emphasis.

Fig. 5 shows the achieved capacities as a function of transmission distance for the MZM (Fig. 5a), PFL (Fig. 5b), and DML (Fig. 5c). All the data are shown for signal bandwidths of 2.5 (green-triangle), 5 (red-circle), and 8 (blue-square) GHz, respectively. The results are also summarized in Table 1. With all the three transmitters the back-to-back capacities of 19, 35, and 44 Gbit/s were achieved with signal bandwidths of 2.5, 5, and 8 GHz, respectively. However, after the dispersive propagation, we can see different capacities obtained for the three transmitters. The MZM generates a chirp-free signal and thus, as expected, shows the highest capacities. It is worth noting that after 75 km transmission any increase in the modulation bandwidth beyond 5 GHz brings negligible benefit in terms of capacity. Similarly to the MZM, the benefit of using a larger bandwidth signal decreases with the increased

TABLE I
CAPACITY ACHIEVED AFTER TRANSMISSION

| Distance (km) | Modulator | Achieved capacity (Gbit/s) with different signal bandwidth | | |
|---|---|---|---|---|
| | | 2.5 GHz | 5 GHz | 8 GHz |
| 50 | MZM | 19 | 35 | 44 |
| | PFL | 14 | 23 | **29** |
| | DML | 14 | 22 | **28** |
| 75 | MZM | 18 | 32 | 34 |
| | PFL | 13 | 19 | **25** |
| | DML | 13 | 21 | **25** |
| 125 | MZM | 17 | 28 | 29 |
| | PFL | 10 | 14 | 16 |
| | DML | 12 | 19 | **22** |

transmission distance also for PFL and DML. However, here the achieved capacities drop faster after transmission due to the modulation frequency chirp. Comparison of the three transmitters with 8-GHz DMT signal is plotted in Fig. 6. It clearly shows that the PFL and DML achieve similar performance to the MZM at back-to-back whereas after transmission the capacity achieved using PFL and DML were smaller than that using the MZM. After transmission over 50 km and 75 km of SMF-28, capacities of 28 and 25 Gbit/s were achieved, respectively, using both lasers with a DMT signal of 8 GHz bandwidth. Even after 125 km of dispersive propagation, we achieved a capacity of 22 Gbit/s, again with a signal bandwidth as small as 8 GHz for the DML (and no in-line amplification). This is a factor of two higher capacity than that of the chirp-managed laser (with the more complex transmitter architecture), which reaches 10 Gbit/s using the duobinary modulation format [24].

Up to 75 km the DML showed comparable results to the PFL. However, for larger distances the DML (although of smaller modulation bandwidth and simpler structure) clearly allowed for higher capacities. Another difference observed was how the obtained capacity scales with the signal bandwidth used. For the PFL, the capacity after 75 km keeps dropping as the transmission distance increases. Increasing the modulation bandwidth brings negligible capacity enhancement (e.g., after 150 km, it increases from 9 to 11 Gbit/s when increasing the

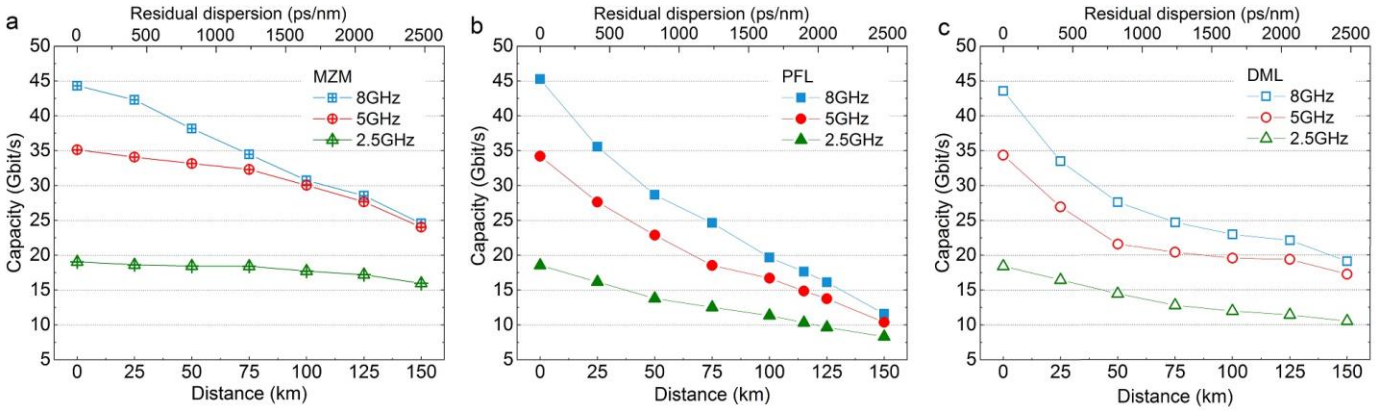


Fig.5. Achieved capacity after transmission using different transmitters: (a) Push-pull $LiNbO_3$ MZM;(b) Directly modulated PFL; (c) Directly modulated DML.

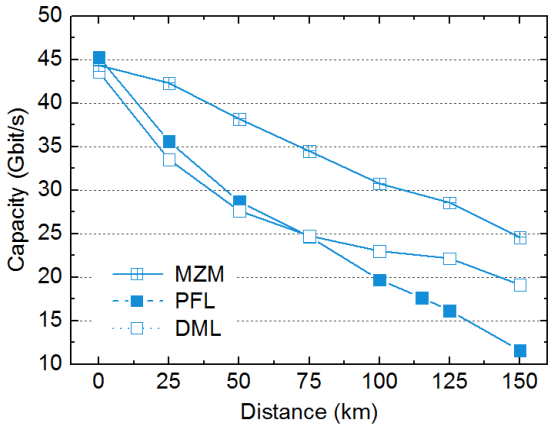


Fig. 6. Capacity obtained for 8-GHz DMT signal with different transmitters.

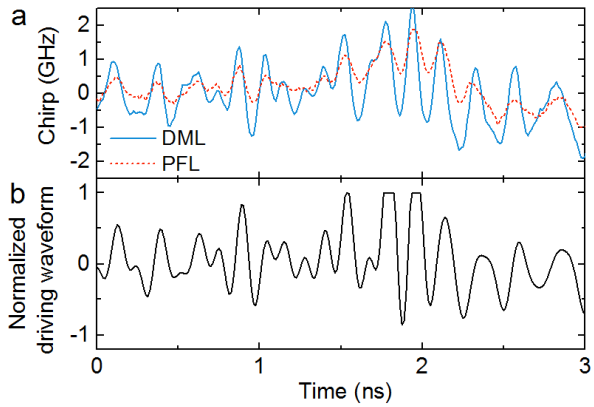


Fig.7 (a) Measured chirp of the DML (solid blue line) and PFL (dashed red line); (b) normalized electrical driving waveform.

signal bandwidth from 2.5 GHz to 8 GHz). For the DML, the capacity after 75 km drops more slowly than the PFL. Here the benefit of using larger bandwidth is more significant, e.g., from 11 Gbit/s to 18 Gbit/s when the signal bandwidth is increased from 2.5 to 5 GHz even after the longest propagation distance of 150 km. Another i nteresting observation is that for distances beyond 100 km, the capacity obtained with the DML is only 20% below that obtained with the MZM, highlighting its small modulation chirp.

Fig. 7a shows the measured modulation chirp (instantaneous frequency deviation) of the DMT waveform (shown in Fig. 7b) as a function of time for both PFL and DML. The chirp was measured using a delayed line interferometer with a delay of 25 ps as an optical frequency discriminator [25]. For both lasers, the chirp value changes proportionally to the driving waveform, suggesting that the chirp was predominantly adiabatic [26]. The DML chirp (measured to be less than ±2.5 GHz) is smaller than that of a standard DFB laser [22,25]. As for the PFL, it had even smaller modulation chirp than the DML (we believe this is thanks to its internal optical feedback). As the chirp of PFL is smaller than that of the DML, the interplay between the chirp and chromatic dispersion cannot explain the poorer performance of the PFL in respect to the DML for propagation distances beyond 75 km. This, however, can be understood by observing the normalized electrical (RF) spectra of the detected signals, which are shown in Fig. 8. Here,

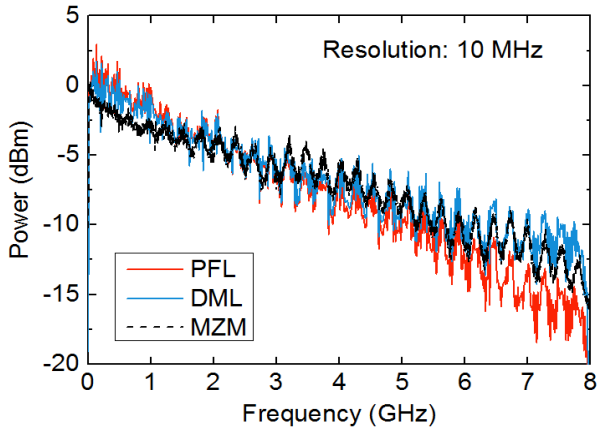


Fig. 8 Electrical spectrum of the detected signals at back-to-back.

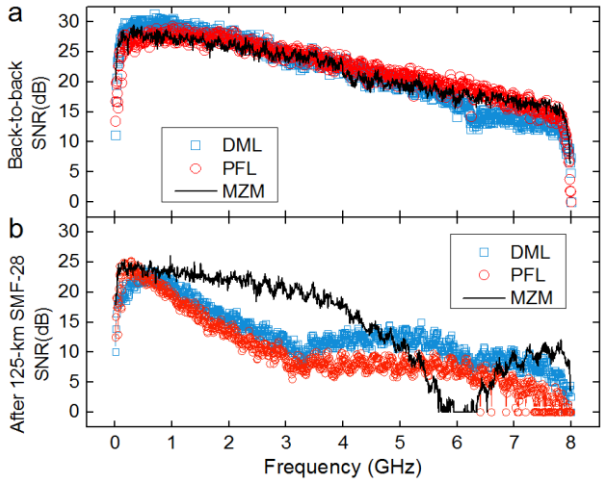


Fig. 9. SNR of the demodulated subcarriers (a) back-to-back; (b) after 125-km transmission.

we clearly see that PFL has a faster frequency roll-off from 4 GHz to 8 GHz while the DML and MZM have flatter frequency response. This signal frequency roll-off causes high-frequency signal components to have relatively smaller power spectral density and thus suffering from the large attenuation due to the propagation through a long (>75 km) length of the optical fiber, causing SNR degradation.

Fig. 9 shows the SNR of the demodulated subcarriers for all three transmitters (PFL, DML, and MZM for comparison): back-to-back is shown in Fig. 9a and after 125-km transmission in Fig. 9b. For the back-to-back case all three transmitters show similar performance, where the SNR smoothly decreases with increased frequency. After 125-km propagation through the SMF-28, the MZM-generated signal has a dip at around 6 GHz due to the dispersion-induced frequency fading. The signal strength around this frequency dip is close to zero (giving SNR=0), confirming that we deal with a purely amplitude modulated signal (without any 'parasitic' phase modulation). For PFL and DML, we see the first frequency-fading dip at a lower frequency as compared to the MZM (around 3.2 GHz), confirming the signal occupies a larger bandwidth (due to the modulation chirp). We also see the second dispersion-induced dip which is close to 6.5 GHz. In contrast to the MZM result, the dispersion-fading induced dips are significantly shallower for the two lasers. The limited depth of the dispersion-induced

dips suggests we have a mixture of amplitude and phase modulation, which is indeed expected from directly-modulated lasers (due to the modulation chirp). The PFL and DML results have similar trend except that the DML has 3-5dB higher SNR at higher frequencies. As we explained earlier, this is due to the frequency roll off of PFL laser modulation response, resulting in limited power of the high-frequency sub-channels.

## V. Discussion

It is worth mentioning that in our experiments a smaller capacity was achieved as compared to the best published back-to-back results [3], as our hardware was different (e.g., the AWG used had only one third of the sampling rate (24 GS/s compared to the 65 GS/s used in [3,4]). This, however, does not pose any limitation to our analysis and conclusions, which deal mainly with limitations due to the DAC resolution, computation complexity, and chromatic dispersion. Also we have already shown in our previous research [13] that the use of a modulation bandwidth beyond 8 GHz does not bring any significant benefit due to dispersion-induced frequency fading for SMF-28 transmission over 50 km and this is also confirmed by our work reported here. Thus the use of a lower-bandwidth DAC is more appropriate in relatively long distance transmission as it reduces power consumption and cost. Additionally, using components with a smaller signal bandwidth generally results in better component performance within their modulation bandwidths. Our results also show that frequency roll-off leads to a limited capacity as well as transmission distance, even with a low-chirp laser. As we conclude that the optimum modulation bandwidth is below 10 GHz, we can foresee further savings in system cost – as suggested in Fig. 8. First, the input directly modulated signal can be amplified by a 10-GHz SOA (rather than an EDFA). At the receiver side, a 10-GHz telecom-grade avalanche photodiode (APD) could be used, eliminating the need for the receiver-side optical pre-amplifier and possibly also the need for the transmitter-side optical amplifier (EDFA or SOA). For example, commercially available APDs receive error-free (BER<$10^{-12}$) OOK 10 Gbit/s signals with a received power as low as -26 dBm [27].


Fig. 10. Our envisaged system architecture: repeater-less, and filter-less transmission through SMF-28.

The technique discussed in this paper can find immediate applications in the 25 Gb/s Ethernet (25 GbE), giving an ample capacity margin for practical application based on 100GBASE-LR4 and 100GBASE-ER4 standard [9]. Another potential application is in the field of cost-sensitive mobile front haul, which targets 25 Gb/s capacity per channel for a transmission distance of up to 20 km [28].

## VI. Conclusion

The performance of the DMT format in a DM-DD system for >50 km repeater-less transmission distance is experimentally studied. Our back-to-back optimization suggests that a 6-bit DAC and 1024 subcarriers offer a reasonable tradeoff (~5% capacity drop) when compared to the corresponding values set for each parameter for maximized capacity. Two different types of directly modulated lasers (PFL and DML) were tested and their performance compared with that obtained using a $LiNbO_3$ MZM in a repeater-less transmission of up to 150 km SMF-28. Using the DML we obtained 25 Gbit/s and 22 Gbit/s raw capacities after 75 and 125 km transmission with a DMT signal of just 8-GHz bandwidth. Such a bandwidth can be easily supported by an avalanche photodiode or fast semiconductor optical amplifier, allowing for EDFA-less operation. Our results may serve as a useful basis for practical considerations of the trade-offs between system performance and component parameters for minimizing the cost-per-bit in DMT transmission beyond 50 km.

## References


[1] IHS Infonetics 10G/40G/100G Telecom Optics Market Size and Forecasts: April 2015.

[2] J.C. Rasmussen, et al., "Digital Signal Processing for Short Reach Optical Links," in Proc. ECOC 2014, Cannes, 2014, Paper Tu.1.3.3.

[3] T. Tanaka, et al., "Experimental investigation of 100-Gbps Transmission over 80-km Single Mode Fiber using Discrete Multi-tone Modulation," in Proc. SPIE 8646(86460J-1), 2012.

[4] W. Yan, et al., "80 km IM-DD Transmission for 100 Gb/s per Lane Enabled by DMT and Nonlinearity Management," in Proc. OFC 2014, San Francisco, 2014, Paper M2I.4.

[5] C. Xie, et al., "Single-VCSEL 100-Gb/s Short-Reach System Using Discrete Multi-Tone Modulation and Direct Detection," in Proc. OFC 2015, Los Angeles, 2015, Paper Tu2H.2.

[6] W.A. Ling, et al., "Single-Channel 50G and 100G Discrete Multitone Transmission With 25G VCSEL Technology," *IEEE/OSA J. Lightwave Technol.*, vol. 33, no. 4, pp. 761–767, Feb. 2015.

[7] Z. Liu, et al., "High-Capacity Directly Modulated Optical Transmitter for 2-μm Spectral Region," *IEEE/OSA J. Lightwave Technol.*, vol. 33, no. 7, pp. 1373–1379, Apr. 2015.

[8] Y. Matsui, et al., "112-Gb/s WDM link using two Directly Modulated Al-MQW BH DFB Lasers at 56 Gb/s," in Proc. OFC 2015, Los Angeles, 2015, Paper Th5B.6.

[9] C. Cole, "Beyond 100 G client optics," *IEEE Commun. Magazine*, vol. 50, no. 2, pp. 58–66, Feb. 2012.

[10] "40Gb/s and 100Gb/s Ethernet Task Force," IEEE P802.3ba. [Online]. Available: http://www.ieee802.org/3/ba/

[11] K. Szczerba, et al., "70 Gbps 4-PAM and 56 Gbps 8-PAM Using an 850 nm VCSEL," *IEEE/OSA J. Lightwave Technol.*, vol. 33, no. 7, pp. 1395–1401, Apr. 2015.

[12] J.C. Cartledge, et al., "100 Gb/s Intensity Modulation and Direct Detection," *IEEE/OSA J. Lightwave Technol.*, vol. 32, no. 16, pp. 2809-2814, 2014.

[13] Z. Liu, et al., "Practical Considerations on Discrete Multi-tone Transmission for Cost-effective Access Networks," in Proc. OFC 2015, Los Angeles, 2015, Paper M3J.4.

[14] Y. Chen, et al., "Demonstration of an 11km Hollow Core Photonic Bandgap Fiber for Broadband Low-latency Data Transmission," in Proc. OFC 2015, Los Angeles, 2015, Paper Th5A.1.

[15] D. G. Nairn, "Time-interleaved analog-to-digital converters," CICC 2008, pp. 289-296, 2008

[16] C. DeCusatis, "Optical Interconnect Networks for Data Communications," *IEEE/OSA J. Lightwave Technol.*, vol. 32, no. 4, pp. 544-552, 2014.

[17] J. Kreissl, et al., "Up to 40-Gb/s Directly Modulated Laser Operating at Low Driving Current: Buried-Heterostructure Passive Feedback Laser (BH-PFL)," *IEEE Photon. Tech. Lett.*, Vol. 24, no. 5, pp. 362-364, 2012.

[18] J. O'Carroll, et al., "Wide temperature range 0 < T < 85 °C narrow linewidth discrete mode laser diodes for coherent communications applications," *Opt. Express*, Vol. 19, no. 26, p. B90-B95, 2011.

[19] B. Kelly, et al., "Discrete mode laser diodes with very narrow linewidth emission," *Electron. Lett.*, vol. 43, no.23, pp. 1282-1284, 2007.

[20] P. Chow, et al., “A Practical Discrete Multitone Transceiver Loading Algorithm for Data Transmission over Spectrally Shaped Channels,” *IEEE Trans. Commun*., Vol. 43, no. 2/3/4, pp.773-775, 1995.
[21] A. M. Wyglinski, et al., “Bit loading with BER-constraint for multicarrier systems,” *IEEE Trans. Wireless Commun.* vol. 4, no. 4, pp. 1383 – 1387, 2005.
[22] P. M. Anandarajah, et al., “Generation of Coherent Multicarrier Signals by Gain Switching of Discrete Mode Lasers,” *IEEE Photon. J*., vol. 3, no. 1, pp. 112-122, 2011.
[23] H Yang, et al., "47.4 Gb/s Transmission Over 100 m Graded-Index Plastic Optical Fiber Based on Rate-Adaptive Discrete Multitone Modulation," *IEEE/OSA J. Lightwave Technol*., vol.28, no.4, pp.352-359, Feb., 2010.
[24] D. Mahgerefteh, et al., “Chirp Managed Laser and Applications,” *IEEE J. Sel. Topics Quantum Electron*., vol. 16, no. 5, pp. 1126 – 1139, 2010.
[25] R.A. Saunders, et al., “Wideband chirp measurement technique for high bit rate sources,” vol. 30, no.16, pp. 1336 – 1338, 1994.
[26] B. W. Hakki. “Evaluation of Transmission Characteristics of Chirped DFB Lasers in Dispersive Optical Fiber”, *IEEE/OSA J. Lightwave Technol*., vol. 10, no.7, pp. 964 – 970, 1992.
[27] T. Nakata, et al., “10Gbit/s high sensitivity, low-voltage operation avalanche photodiodes with thin InAlAs multiplication layer and waveguide structure,” *Electron. Lett*., vol. 36, no. 24, pp. 2033-2034, 2000.
[28] N. Deng, et al. “WDM Solutions and Technologies for Mobile Fronthaul,” in Proc. ACP 2015, Hong Kong, 2015, paper ASu3G.2.